

University of Groningen

**Pharmacokinetics of a sustained release formulation of PDGF $\beta$ -receptor directed carrier proteins to target the fibrotic liver**

van Dijk, F.; Teekamp, N.; Beljaars, L.; Post, E.; Zuidema, J.; Steendam, R.; Kim, Y. O.; Frijlink, H. W.; Schuppand, D.; Poelstra, K.

*Published in:*  
Journal of Controlled Release

*DOI:*  
[10.1016/j.jconrel.2017.11.029](https://doi.org/10.1016/j.jconrel.2017.11.029)

**IMPORTANT NOTE: You are advised to consult the publisher's version (publisher's PDF) if you wish to cite from it. Please check the document version below.**

*Document Version*  
Publisher's PDF, also known as Version of record

*Publication date:*  
2018

[Link to publication in University of Groningen/UMCG research database](#)

*Citation for published version (APA):*

van Dijk, F., Teekamp, N., Beljaars, L., Post, E., Zuidema, J., Steendam, R., Kim, Y. O., Frijlink, H. W., Schuppand, D., Poelstra, K., Hinrichs, W. L. J., & Olinga, P. (2018). Pharmacokinetics of a sustained release formulation of PDGF $\beta$ -receptor directed carrier proteins to target the fibrotic liver. *Journal of Controlled Release*, 269, 258-265. <https://doi.org/10.1016/j.jconrel.2017.11.029>

**Copyright**

Other than for strictly personal use, it is not permitted to download or to forward/distribute the text or part of it without the consent of the author(s) and/or copyright holder(s), unless the work is under an open content license (like Creative Commons).

The publication may also be distributed here under the terms of Article 25fa of the Dutch Copyright Act, indicated by the "Taverne" license. More information can be found on the University of Groningen website: <https://www.rug.nl/library/open-access/self-archiving-pure/taverne-amendment>.

**Take-down policy**

If you believe that this document breaches copyright please contact us providing details, and we will remove access to the work immediately and investigate your claim.

Downloaded from the University of Groningen/UMCG research database (Pure): <http://www.rug.nl/research/portal>. For technical reasons the number of authors shown on this cover page is limited to 10 maximum.



## Pharmacokinetics of a sustained release formulation of PDGF $\beta$ -receptor directed carrier proteins to target the fibrotic liver

F. van Dijk<sup>a,b,1</sup>, N. Teekamp<sup>a,1</sup>, L. Beljaars<sup>b</sup>, E. Post<sup>b</sup>, J. Zuidema<sup>c</sup>, R. Steendam<sup>c</sup>, Y.O. Kim<sup>d</sup>, H.W. Frijlink<sup>a</sup>, D. Schuppan<sup>d,e</sup>, K. Poelstra<sup>b</sup>, W.L.J. Hinrichs<sup>a,\*</sup>, P. Olinga<sup>a</sup>

<sup>a</sup> Groningen Research Institute of Pharmacy, Department of Pharmaceutical Technology and Biopharmacy, University of Groningen, Groningen, The Netherlands

<sup>b</sup> Groningen Research Institute of Pharmacy, Department of Pharmacokinetics, Toxicology and Targeting, University of Groningen, The Netherlands

<sup>c</sup> InnoCore Pharmaceuticals, Groningen, The Netherlands

<sup>d</sup> Institute of Translational Immunology, Research Center for Immune Therapy, University Medical Center, Johannes Gutenberg University, Mainz, Germany

<sup>e</sup> Beth Israel Deaconess Medical Center, Harvard Medical School, Boston, MA, USA

### ARTICLE INFO

#### Keywords:

Controlled release  
Biodegradable polymeric microspheres  
PDGF $\beta$ -receptor targeted drug carrier  
Protein delivery  
*in vitro in vivo* correlation  
Liver fibrosis

### ABSTRACT

Liver fibrogenesis is associated with excessive production of extracellular matrix by myofibroblasts that often leads to cirrhosis and consequently liver dysfunction and death. Novel protein-based antifibrotic drugs show high specificity and efficacy, but their use in the treatment of fibrosis causes a high burden for patients, since repetitive and long-term parenteral administration is required as most proteins and peptides are rapidly cleared from the circulation. Therefore, we developed biodegradable polymeric microspheres for the sustained release of proteinaceous drugs. We encapsulated the drug carrier pPB-HSA, which specifically binds to the PDGF $\beta$ R that is highly upregulated on activated myofibroblasts, into microspheres composed of hydrophilic multi-block copolymers composed of poly(L-lactide) and poly ethylene glycol/poly( $\epsilon$ -caprolactone), allowing diffusion-controlled release. Firstly, we estimated in mice with acute fibrogenesis induced by a single CCl<sub>4</sub> injection the half-life of <sup>125</sup>I-labeled pPB-HSA at 40 min and confirmed the preferential accumulation in fibrotic tissue. Subsequently, we determined in the Mdr2<sup>-/-</sup> mouse model of advanced biliary liver fibrosis how the subcutaneously injected microspheres released pPB-HSA into both plasma and fibrotic liver at 24 h after injection, which was maintained for six days. Although the microspheres still contained protein at day seven, pPB-HSA plasma and liver concentrations were decreased. This reduction was associated with an antibody response against the human albumin-based carrier protein, which was prevented by using a mouse albumin-based equivalent (pPB-MSA). In conclusion, this study shows that our polymeric microspheres are suitable as sustained release formulation for targeted protein constructs such as pPB-HSA. These formulations could be applied for the long-term treatment of chronic diseases such as liver fibrosis.

### 1. Introduction

Sustained release drug delivery systems are increasingly used as a patient-friendly alternative to conventional dosage forms [1,2]. When controlling the release rate of a drug its therapeutic actions can be drastically improved by obtaining prolonged release associated with less fluctuations in plasma concentration. This avoids peak levels and reduces side effects. This way, the bioavailability, efficacy and safety of drugs can be significantly enhanced [2,3]. One such drug delivery system is microspheres, that allows flexible dosing of the drug [4]. This approach is particularly interesting for application of potent protein-based therapeutics, as the administration frequency can be largely

reduced as compared to intravenous administration. Moreover, when encapsulated in polymeric microparticles, the biopharmaceutical can be effectively protected from degradation induced by biological conditions or enzymes [2,5].

In the treatment of chronic diseases such as fibrosis, the application of sustained release formulations like microspheres for antifibrotic drugs could significantly improve patient compliance and therapeutic efficacy, especially since the expected treatment would be long-term. Hepatic fibrosis is a progressive, pathological condition affecting millions of people worldwide [6]. Following chronic liver injury, inflammatory and bile ductular cells release a variety of mediators that provoke the activation of fibroblasts and hepatic stellate cells to

\* Corresponding author at: University of Groningen, Department of Pharmaceutical Technology and Biopharmacy, A. Deusinglaan 1, 9713 AV Groningen, The Netherlands.  
E-mail address: [w.l.j.hinrichs@rug.nl](mailto:w.l.j.hinrichs@rug.nl) (W.L.J. Hinrichs).

<sup>1</sup> The authors contributed equally.

myofibroblasts, which start to produce extracellular matrix (ECM) components, especially fibrillar collagens in a chronic wound healing reaction. In cirrhosis, which represents an advanced stage of fibrosis, the liver vascular architecture gets progressively distorted and functional parenchymal cells are ultimately replaced by abundant ECM, which causes liver failure, and finally decompensated cirrhosis [7–9].

For some patients with cirrhosis, liver transplantation or treatment with a new generation of highly effective antiviral agents against Hepatitis B and C may be a curative treatment, however there is still an urge for effective antifibrotic treatments to fulfill the needs of all patients [10–12]. Many promising new drugs are biological-based, such as growth factors, cytokines and monoclonal antibodies. A class of therapeutic proteins currently under development is the fusion proteins, including biologic-based drugs modified with targeting moieties [13,14]. Such proteins are particularly interesting as their therapeutic effects can be increased while avoiding side effects [15]. The platelet-derived growth factor beta receptor (PDGFR) is abundantly expressed on myofibroblasts in fibrotic tissues with high fibrogenic activity [16,17], and therefore its expression was exploited as a potential target for the cell-specific delivery of antifibrotic drugs. A carrier protein with high affinity for the PDGFR was designed, composed of an albumin core with multiple cyclic PDGFR-recognizing peptides (pPB) binding the PDGFR. Previous studies have shown that the carrier, referred to as pPB-HSA, selectively bound to the PDGFR and accumulated in fibrogenic cells in the fibrotic liver which highly expressed the PDGFR. The carrier itself did neither elicit an antifibrotic effect nor induced proliferation of fibroblasts [18].

Because many therapeutic proteins have poor *in vivo* pharmacokinetic properties as reflected by relatively short *in vivo* plasma half-lives, we developed a microsphere formulation containing pPB-HSA that ensures gradual protein release over a period of 14 days, which could be suitable for therapeutic application of other large therapeutic proteins as well. A blend of two biodegradable semi-crystalline multi-block co-polymers, composed of crystalline blocks of poly(L-lactide) (PLLA) and amorphous blocks of poly ethylene glycol (PEG) and poly( $\epsilon$ -caprolactone) (PCL), was used as a matrix for these microspheres. Whilst mostly polymers are used that show degradation-controlled release [19], e.g. poly (lactic-co-glycolic acid), these particular polymers provided diffusion-controlled release of proteins, caused by swelling of the PEG blocks by water uptake [20]. Disadvantage of degradation-controlled release is that the degradation products of the polymer are usually incompatible with proteins [21].

We previously showed proof of concept of effective release of drug carriers from microspheres composed of these multi-block copolymers in the unilateral ureter obstruction model for kidney fibrosis. In that study, we demonstrated the release of pPB-HSA from subcutaneously injected microspheres into plasma and the subsequent localization of this drug carrier in the fibrotic kidney 7 days after administration of the microspheres [22]. Although we were able to demonstrate protein release after 7 days, the *in vivo* release characteristics and the correlation with the *in vivo* kinetics remained undefined.

In the present study, we therefore further explored the applicability of these microspheres as a sustained controlled release formulation for biologicals. For this, we examined the *in vivo* kinetic behavior of pPB-HSA in two different mouse models for liver fibrosis that display high and specific PDGFR-expression, i.e. the acute CCl<sub>4</sub> model and the Mdr2<sup>−/−</sup> model. In the acute CCl<sub>4</sub> model, we used I<sup>125</sup>-labeled pPB-HSA to determine pharmacokinetic parameters and tissue distribution of this carrier protein. Subsequently, the *in vivo* release profile of pPB-HSA from microspheres was determined in the chronic Mdr2<sup>−/−</sup> model.

## 2. Materials and methods

### 2.1. Pharmacokinetics of I<sup>125</sup>-labeled pPB-HSA

The experimental protocols for animal studies with the CCl<sub>4</sub>-model were approved by the Animal Ethical Committee of the University of Groningen (The Netherlands). Male C57BL/6 mice (20–22 g) were obtained from Envigo (Horst, The Netherlands). Animals received *ad libitum* normal diet with a 12 h light/dark cycle. Mice ( $n = 12$ ) received a single injection of CCl<sub>4</sub> (Sigma Aldrich, Zwijndrecht, The Netherlands) diluted in olive oil (0.5 mg/kg) intraperitoneally. After 24 h, mice were intravenously injected with tracer amounts of I<sup>125</sup>-labeled pPB-HSA ( $1 \times 10^5$ – $5 \times 10^5$  counts per minute (CPM) in PBS) and sacrificed after 10, 30 or 60 min ( $n = 4$  per time point), after which blood and all organs were collected to assess radioactivity [18]. pPB-HSA was labeled with I<sup>125</sup> as described before [18].

### 2.2. Synthesis of polymers and proteins

The two multi-block co-polymers were synthesized as described before from the prepolymers PLLA and PCL-PEG-PCL [22,23]. In short, [PLLA] was chain-extended with [PCL-PEG<sub>1000</sub>-PCL or PCL-PEG<sub>3000</sub>-PCL] using 1,4-butanediisocyanate (Actu-all Chemicals B.V., Oss, The Netherlands), to prepare the multi-block co-polymers [PCL-PEG<sub>1000</sub>-PCL]-[PLLA] (50/50 weight ratio) and [PCL-PEG<sub>3000</sub>-PCL]/[PLLA] (30/70 weight ratio). For this, [PLLA] and [PCL-PEG<sub>1000</sub>-PCL or PCL-PEG<sub>3000</sub>-PCL] were dissolved in dry 1,4-dioxane (80 °C, 30 wt-% solution), 1,4-butanediisocyanate was added and the reaction mixture stirred for 20 h. The reaction mixture was frozen and freeze-dried at 30 °C shelf temperature to remove 1,4-dioxane.

The proteins pPB-HSA and pPB-MSA were synthesized as described before [24]. Briefly, *N*- $\gamma$ -maleimidobutyl-oxy-succinimide ester was added to either human (purified from Cealb®, Sanquin, Amsterdam, The Netherlands) or mouse serum albumin (Equitech-Bio Inc., Kerville, TX, USA). Next, *N*-succinimidyl *S*-acetylthioacetate (SATA)-modified pPB (C\*SRNLIDC\*, Ansynth Service B.V., Roosendaal, The Netherlands) and activation solution (containing hydroxylamine and EDTA) were added. After extensive dialysis, the monomeric product was freeze-dried and stored at  $-20$  °C.

### 2.3. Production and characterization of microspheres

Microspheres were produced using a similar water-in-oil-in-water double emulsification evaporation method as described previously [22]. In brief, the multi-block co-polymers were dissolved in dichloromethane in a 50:50 weight ratio. For the primary emulsion, PBS (control) or a solution of 80 mg/mL protein (HSA; or pPB-HSA and HSA, or the mouse equivalents, in a 3:2 ratio) was added to the filtered polymer solution to obtain 5 wt-% theoretical protein load and homogenized. For the secondary emulsion, the primary emulsion was added to 4 wt-% poly vinyl alcohol (Sigma Aldrich) + 5 wt-% NaCl solution in water under stirring. The hardened microspheres were collected by filtration, washed and freeze dried.

Microspheres were characterized for morphology by scanning electron microscopy, for particle size distribution by laser diffraction, and for protein content and *in vitro* release of HSA, pPB-HSA or pPB-MSA as described by [22]. Scanning electron microscopy imaging was performed at an acceleration voltage of 10 kV (JSM-6460 microscope, Jeol, Tokio, Japan). Samples were fixed on an aluminum sample holder using double sided adhesive carbon tape and sputter coated with 10 nm of gold. The particle size distributions of microspheres were determined with laser diffraction and subsequently the span of the particle size distribution was calculated using Eq. (1),

$$\text{Span} = \frac{X_{10} - X_{90}}{X_{50}} \quad (1)$$

where  $X_{10}$ ,  $X_{50}$  and  $X_{90}$  represent the volume percentages of particles (10%, 50% and 90% undersize, respectively). The *in vitro* release was measured in triplicate by a sample-and-replace method. Briefly, 10 mg of microspheres were suspended in 1.0 mL release buffer (100 mM sodium phosphate buffer, containing NaCl, Tween 80 and  $\text{NaN}_3$ ). Samples of 800  $\mu\text{L}$  were taken at predetermined time points and replaced by fresh buffer. Protein concentrations were determined with BCA assay and an in-house developed ELISA for pPB-HSA (see section ELISA). The protein content of the remaining microspheres was determined using BCA assay as described before [22] and was used to calculate the encapsulation efficiency (EE), which is defined as the weight of encapsulated protein (i.e. HSA, pPB-HSA or pPB-MSA) divided by the weight of total protein used.

## 2.4. Pharmacokinetics of pPB-HSA from microspheres

Studies with the *Mdr2*<sup>−/−</sup> mouse model were approved by the Animal Ethical Committee of the State of Rhineland Palatinate. Female FVB mice ( $n = 8$ ) were obtained from Jackson Laboratory (Jackson Laboratory, Bar Harbor, ME, USA) and FVB *Mdr2*<sup>−/−</sup> mice ( $n = 24$ ) (20–28 g) were bred in homozygosity at the Institute of Translational Immunology at Mainz University Medical Center. *Mdr2*<sup>−/−</sup> mice aged 11–15 weeks display advanced liver fibrosis with a 4 to 5-fold increased liver collagen content [25]. Wildtype and *Mdr2*<sup>−/−</sup> mice were housed with a 12 h light/dark cycle with water and *ad libitum* normal diet. At age 11–15 weeks *Mdr2*<sup>−/−</sup> mice were injected subcutaneously in the neck, a site with sufficient subcutaneous space, with a suspension of 12.6 wt-% microspheres in 500  $\mu\text{L}$  0.4% carboxymethyl cellulose (CMC, Aqualon high  $M_w$ , Ashland, pH 7.0–7.4). Microspheres contained either 5 wt-% HSA ( $n = 4$ ), 3 wt-% pPB-HSA + 2 wt-% HSA ( $n = 16$ ), 3 wt-% pPB-MSA + 2 wt-% MSA ( $n = 8$ ), or were empty (polymer only) ( $n = 4$ ). Groups of mice were sacrificed at 1, 3, 5 or 7 days for pPB-HSA microspheres ( $n = 4$  at each time point) and all other groups at day 7 after microsphere administration. Blood, liver and off target organs were collected for further analysis.

## 2.5. ELISA

### 2.5.1. ELISA for pPB-HSA

pPB-HSA levels both *in vitro* (100  $\mu\text{L}$  release buffer) and *in vivo* (100  $\mu\text{L}$  plasma or 1.4 mg/100  $\mu\text{L}$  protein of liver, as determined with Lowry assay) were assessed with our in-house developed sandwich ELISA [22]. In short, the capture antibody  $\alpha$ -pPB was diluted in coating buffer (100 mM  $\text{NaHCO}_3$ /33 mM  $\text{Na}_2\text{CO}_3$  in water (pH 9.5) and incubated overnight (100  $\mu\text{L}$ , 6.5 mg/mL, 1:1000, custom prepared by Charles Rivers, Den Bosch, The Netherlands) in a 96-well high protein binding plate (Corning, New York, NY, USA). The plate was washed extensively with PBS containing 0.5% Tween-20 (PBS-T) and blocked with 200  $\mu\text{L}$  5 wt-% nonfat dry milk in PBS-T for 1 h. After washing, 100  $\mu\text{L}$  sample was incubated for 2 h. The plate was washed again, and the detection antibody goat  $\alpha$ -HSA was applied (100  $\mu\text{L}$ , 1:8000, ICN Biomedicals, Zoetermeer, The Netherlands) for 1 h. The appropriate HRP-conjugated secondary antibody (100  $\mu\text{L}$ , 1:2000, DAKO, Santa Clara, CA, USA) was applied for 1 h, and the substrate tetramethyl benzidine (100  $\mu\text{L}$ , R&D Systems, Minneapolis, MN, USA) was incubated for 20 min after washing with PBS-T. The absorbance was measured at 450 nm (THERMOMax microplate reader, Molecular Devices, Sunnyvale, CA, USA) after addition of 50  $\mu\text{L}$  2 N  $\text{H}_2\text{SO}_4$ .

### 2.5.2. ELISA for immunoglobulins

Plasma levels of immunoglobulins against pPB-HSA or pPB-MSA were measured with an in-house developed ELISA. Either pPB-HSA or pPB-MSA (100  $\mu\text{L}$ , 10  $\mu\text{g}/\text{mL}$  coating buffer) was incubated for 2 h at room temperature in a high protein binding 96-well plate (Corning). After extensive washing with PBS-T, non-specific binding sites were blocked with 200  $\mu\text{L}$  5 wt-% nonfat dry milk in PBS-T for 1 h. Plasma

samples (100  $\mu\text{L}$  plasma, diluted 1:100) were added for incubation of 1 h after washing with PBS-T. The plate was washed again and HRP-conjugated anti-mouse immunoglobulins diluted in blocking buffer (100  $\mu\text{L}$ , 1:2000, DAKO) were incubated for 1 h. After washing with PBS-T, the substrate tetramethyl benzidine (100  $\mu\text{L}$ , R&D Systems) was incubated for 20 min. The absorbance was measured at 450 nm after addition of 50  $\mu\text{L}$  2 N  $\text{H}_2\text{SO}_4$ .

## 2.6. Quantitative real-time PCR

Total RNA from was isolated from livers using a Maxwell® LEV simply RNA Cells/Tissue kit (Promega, Madison, WI, USA) according to manufacturer's instructions. RNA concentrations were determined using NanoDrop ND-100 spectrophotometer (NanoDrop Technologies, Wilmington, DE, USA). The primers used include procollagen  $\alpha 1(\text{I})$  forward: 5'-TGACTGGAAGACGGAGAGT-3'; reverse: 3'-ATCCATCGGTCATGCTCTCT-5'; PDGF $\beta$ -receptor forward: 5'-AACCCCTTACAGCTGTCCT-3'; reverse: 3'-TTCCTCTATTGCCATCTC-5';  $\beta$ -actin forward: 5'-ATCGTGCCTGACATCAAAGA-3'; reverse: 3'-ATGCCACAGGATTCCATACC-5' (all Sigma-Aldrich). Quantitative real-time PCR analysis was performed with 10 ng cDNA per sample according to manufacturer's instructions (SensiMix™ SYBR kit, Bioline, Taunton, MA, USA) and was analyzed by the ABI7900HT sequence detection system (Applied Biosystems, Foster City, CA, USA). For each sample, the threshold cycles (Ct values) were calculated with the SDS 2.3 software program (Applied Biosystems) and mRNA expression was normalized for  $\beta$ -actin.

## 2.7. Immunohistochemistry

Cryosections of neck skin tissue were cut with a thickness of 4  $\mu\text{m}$  (CryoStar NX70 cryostat, Thermo Fisher Scientific), dried and fixed with acetone. Paraffin sections of livers were cut with a Leica Reichert-Jung 2040 microtome (Leica Microsystems, Nussloch, Germany) with a thickness of 4  $\mu\text{m}$ . The sections were deparaffinized in xylene and ethanol. All sections were rehydrated in PBS and were incubated for 1 h with the primary antibody (goat anti-collagen I&III (both 1:200 + 5% normal mouse serum (Southern Biotech, Birmingham, AL, USA)) or rabbit anti-HSA (1:1500 (ICN Biomedicals)) at room temperature or boiled in 10 mM Tris/1 mM EDTA (pH 9.0) for 15 min prior to overnight incubation with rabbit anti-PDGF $\beta$ -receptor (1:50, Cell Signaling) at 4 °C. Next, sections were incubated with the appropriate HRP-conjugated secondary antibody (1:100, DAKO, Santa Clara, CA, USA) for 30 min at room temperature, which were visualized with ImmPACT NovaRED (both Vector, Burlingame, CA, USA). Hematoxylin counterstaining was performed. Digital photomicrographs were captured at 400 $\times$  magnification (Aperio, Burlingame, CA, USA).

## 2.8. Statistical analyses

At least 3 individual experiments were performed for the *in vitro* microsphere characterization and these data are represented as mean  $\pm$  SD. All other data are represented as mean  $\pm$  SEM. The graphs and statistical analyses were performed with Graphpad Prism version 6.0 (GraphPad Prism Software, Inc., La Jolla, CA, USA). The differences between the groups were assessed by ordinary one-way ANOVA followed by Bonferroni's multiple comparison test unless stated otherwise. Basic pharmacokinetic modeling was performed with the computer program Multifit for non-linear curve-fitting [26].

## 3. Results

### 3.1. In vivo pharmacokinetics of pPB-HSA

To determine the *in vivo* kinetics and tissue distribution of pPB-HSA, all organs of mice with  $\text{CCl}_4$ -induced acute liver fibrogenesis were collected and examined after a single intravenous injection with  $^{125}\text{I}$ -



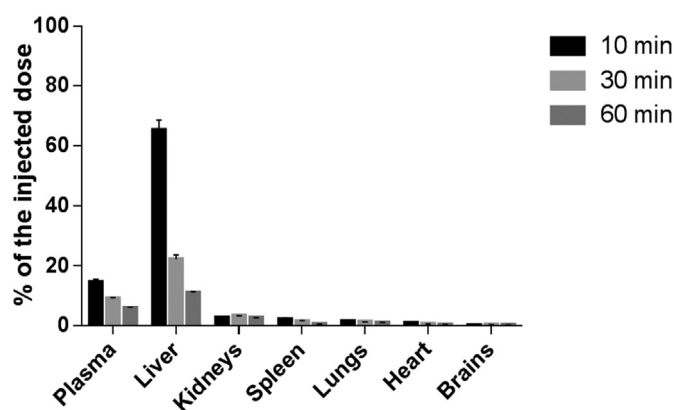


Fig. 1. *In vivo* distribution of  $^{125}\text{I}$ -labeled pPB-HSA in plasma, liver and off-target organs at 10, 30 and 60 min after intravenous injection in mice with  $\text{CCl}_4$ -induced acute liver fibrosis.

labeled pPB-HSA. Ten minutes after injection, high amounts ( $65 \pm 6\%$  of the dose) accumulated in the liver, expressing the PDGFR [15], whereas  $15 \pm 2\%$  was still found in the plasma. A minor amount of the remaining fraction was detected in the kidneys ( $2.6 \pm 0.5\%$ ), spleen ( $2.1 \pm 1.0\%$ ), lungs ( $1.4 \pm 0.5\%$ ), heart ( $0.9 \pm 0.3\%$ ) and brains ( $0.2 \pm 0.1\%$ ). The active targeting of pPB-HSA to myofibroblasts in the fibrotic liver has been shown in previous studies [18], and we herewith confirmed the steering of pPB-HSA to the organ with the highest PDGFR-expression (Fig. 1). Based on the plasma concentration per milliliter at 10, 30 and 60 min after injection, the *in vivo* plasma half-life was calculated to be approximately 40 min. Basic kinetic modeling assuming 1-compartment kinetics further yielded a rough estimate for the clearance of  $58 \mu\text{L}/\text{min}$  and for the volume of distribution of 3 mL (Fig. S1 and Table S1).

### 3.2. Microsphere characterization

Microspheres containing pPB-HSA that ensure gradual and prolonged release into plasma for at least 7 days were developed. All microspheres were spherically shaped and had a smooth surface with little to no pores, as shown with scanning electron microscopy (Fig. 2A, Fig. S2). Laser diffraction analysis revealed that the two batches of protein-loaded microspheres had similar particle size distributions with a median particle size of around  $25 \mu\text{m}$ , while polymer-only control microspheres were slightly smaller at all volume percentages (Table 1). The polydispersity is expressed in the span (Eq. (1)), which is comparable to values found in earlier studies applying the same production process [22]. Both protein-loaded microsphere formulations yielded high encapsulation efficiencies of protein (Table 1) and showed low burst release and sustained release *in vitro* for at least 14 days (Fig. 2B), with a cumulative release after 14 days of 52% for pPB-HSA and 55% for HSA. The slightly higher molecular weight of pPB-HSA ( $\sim 74 \text{ kDa}$ ) than HSA ( $67 \text{ kDa}$ ) did not affect the release rate, with average values of  $4.5 \pm 0.65\%/ \text{day}$  and  $5.0 \pm 0.29\%/ \text{day}$ , respectively.

### 3.3. Pharmacokinetic profile of pPB-HSA released from microspheres *in vivo*

The pPB-HSA microspheres were subcutaneously injected in the neck of  $\text{Mdr2}^{-/-}$  mice with advanced biliary liver fibrosis. These mice exhibit a profound increase in procollagen  $\alpha 1(\text{I})$  and PDGFR gene expression as compared to normal mice (Fig. 3A, D), which is a hallmark of fibrosis [25]. The livers of these  $\text{Mdr2}^{-/-}$  mice showed characteristic deposition of collagen types I & III in the portal areas particularly around the bile ducts (Fig. 3B) as a consequence of the toxicity of accumulated of phosphatidylcholine in the hepatocytes, due to the knock out of the transporter gene. Collagen deposition extended

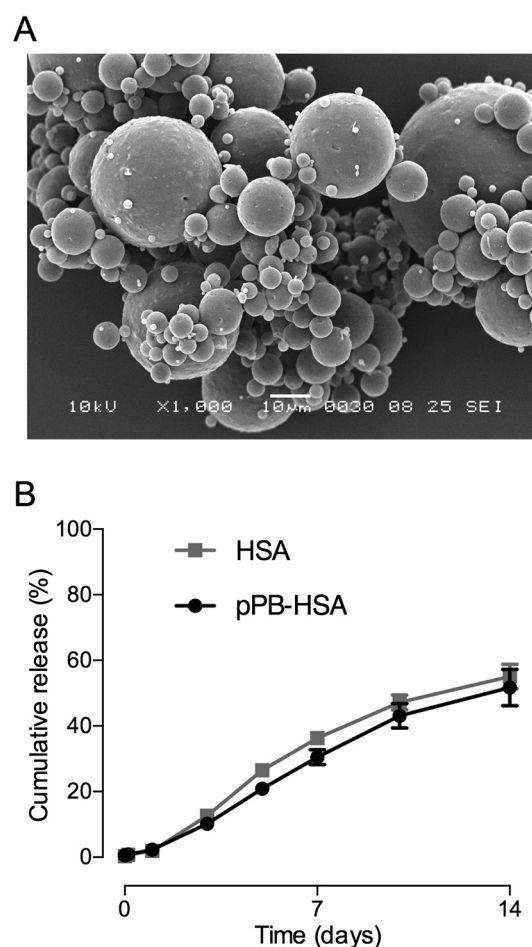


Fig. 2. Morphology and *in vitro* release of pPB-HSA from microspheres used in the  $\text{Mdr2}^{-/-}$  model for liver fibrosis. (A) Representative scanning electron micrograph of pPB-HSA microspheres after freeze-drying ( $1000\times$  magnification). The empty microspheres and microspheres containing HSA only exhibited similar morphology. (B) Cumulative *in vitro* release of pPB-HSA and HSA from pPB-HSA microspheres and HSA microspheres, respectively. Percentages are corrected for EE.

into advanced portal to portal bridge formation in the parenchyma (Fig. 3C). Accordingly, myofibroblasts lining the fibrotic bile ducts and myofibroblasts in the parenchyma expressed the PDGFR (Fig. 3E, F).

The microsphere injection site was inspected for presence and appearance of microspheres that resided for 7 days at the injection site. Clearly, during these 7 days the microspheres remained subcutaneous (Fig. 4A) and the staining for HSA demonstrated that the microspheres *in vivo* still contained protein after 7 days (HSA and pPB-HSA) (Fig. 4B, C), as was expected from the *in vitro* release studies.

The pharmacokinetic profile of the released pPB-HSA was determined at 1, 3, 5 and 7 days after injection. We confirmed sustained release of pPB-HSA from the microspheres into the plasma up to 7 days after injection reaching a steady state concentration of  $44.9 \pm 4.7 \text{ ng/mL}$ , which equals  $2.4 \times 10^{-3} \pm 0.3 \times 10^{-3}\%/ \text{mL}$  based on the total pPB-HSA content of the microspheres, within 1 day after injection and remained constant for 5 days (Fig. 5A). The infusion rate of pPB-HSA from the microspheres into the circulation was determined by multiplying this value with the clearance as estimated in the acute  $\text{CCl}_4$ -model, yielding an infusion rate of 0.2% per day. Interestingly, the steady state concentration in plasma was  $78.5 \pm 10.9\%$  lower at 7 days after injection than at day 5 ( $p < 0.0001$ , unpaired student *t*-test).

In line with the PDGFR-expression, pPB-HSA was present in the fibrotic livers at all time points, reflecting a similar pattern as seen in plasma, reaching a steady state concentration of  $121 \pm 28.3 \text{ ng/}$

**Table 1**  
Characteristics of microspheres with different content as used *in vivo* in the Mdr2<sup>-/-</sup> model.

Formulation	Protein load	Particle size ( $\mu\text{m} \pm \text{SD}$ )			Span	Encapsulation efficiency (%)
		$X_{10}$	$X_{50}$	$X_{90}$		
pPB-HSA	3% pPB-HSA/2% HSA	$4.4 \pm 0.3$	$23.3 \pm 1.5$	$59.5 \pm 5.0$	2.4	99
HSA	5% HSA	$4.1 \pm 0.2$	$27.6 \pm 0.7$	$59.1 \pm 1.2$	2.0	81
Control	–	$2.5 \pm 0.1$	$16.7 \pm 1.2$	$43.9 \pm 0.7$	2.5	–

liver within 1 day after injection (Fig. 5B). Similar to the observations in plasma, a decline of  $75.4 \pm 5.3\%$  in the pPB-HSA concentration was detected in the livers after 7 days as compared to day 5 ( $p = 0.002$ , unpaired student *t*-test). As expected, for both plasma and livers, the control group with microspheres containing HSA only did not show any presence of pPB-HSA.

The *in vivo* reduction in pPB-HSA levels 7 days after injection as compared to earlier time-points was rather unexpected, as protein was still present in the subcutaneous microspheres after 7 days (Fig. 4B and C) and the *in vitro* data showed minimal burst release of pPB-HSA followed by pseudo-zero order sustained release kinetics for 10 to 14 days (Fig. 2B). To further investigate this phenomenon, plasma samples were analyzed for the presence of antibodies against the albumin-based carrier as this is not a mouse based protein, which might interfere with our results. Indeed, the decline in pPB-HSA concentration at day 7 coincided with the induction of an antibody response against pPB-HSA as compared to the empty microspheres as control group. Mice that received microspheres containing HSA only also showed an induction of the immune response to the same extent (Fig. 6A). This immunological reaction in these mice to the drug carrier was completely absent when microspheres contained pPB-MSA, in which human serum albumin was replaced with the mouse equivalent (Fig. 6B), as the response was not exceeding background levels. The pPB-MSA microspheres displayed similar size distribution (median  $22 \mu\text{m}$ ) and morphology, and showed slightly faster *in vitro* release characteristics than

the microspheres containing the human albumin-based carrier (Fig. S3, Table S2).

#### 4. Discussion

Protein-based therapeutics including fusion proteins, such as protein-based drugs modified with targeting moieties, drastically increased the treatment perspective for a wide variety of diseases [13,14,27]. In the past decades, we developed various compounds enriched with PDGF $\beta$ -receptor recognizing peptides (pPB) including the myofibroblast-selective drug carrier PDGF $\beta$ R-targeted human serum albumin (pPB-HSA) [18]. We aim to apply this PDGF $\beta$ R-targeted drug carrier, when coupled to an effective antifibrotic compound, for the treatment of chronic fibrotic diseases. However, delivery of protein-based compounds involves parenteral administration with consequent short-lasting peak-concentrations and the need for frequent application, posing a high burden to the potential patient. For effective treatment of such diseases the sustained release of therapeutics is essential. We therefore developed a patient-friendly formulation providing sustained release of protein therapeutics, which can be applied for protein constructs like pPB-HSA [22]. In the present study, we showed that pPB-HSA was released from the subcutaneous polymeric microspheres into the plasma and reached easily detectable levels in the fibrotic liver, where a steady state concentration was achieved within 1 day after microsphere injection, which lasted for 5 days. A sudden decrease of

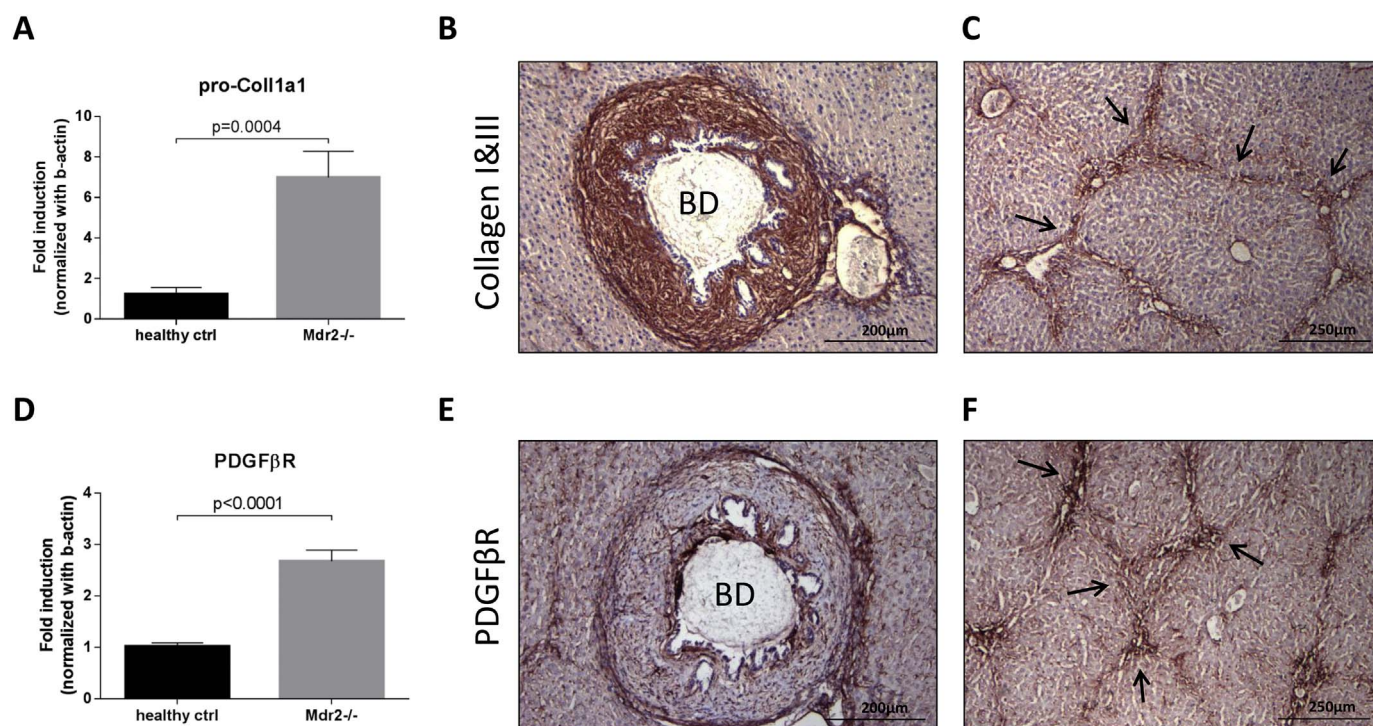


**Fig. 3.** (pro-) Collagen and PDGF $\beta$ -receptor expressions at mRNA (A and D, respectively) and protein level (B, C, E, F) in livers of Mdr2<sup>-/-</sup> mice. Of note, the staining (in red) is observed in particular around the bile ducts (BD) (B and E, respectively) and in the parenchyma (C and F, respectively). Differences between groups were assessed by unpaired student *t*-test. Arrows indicate fibrous collagen bands.



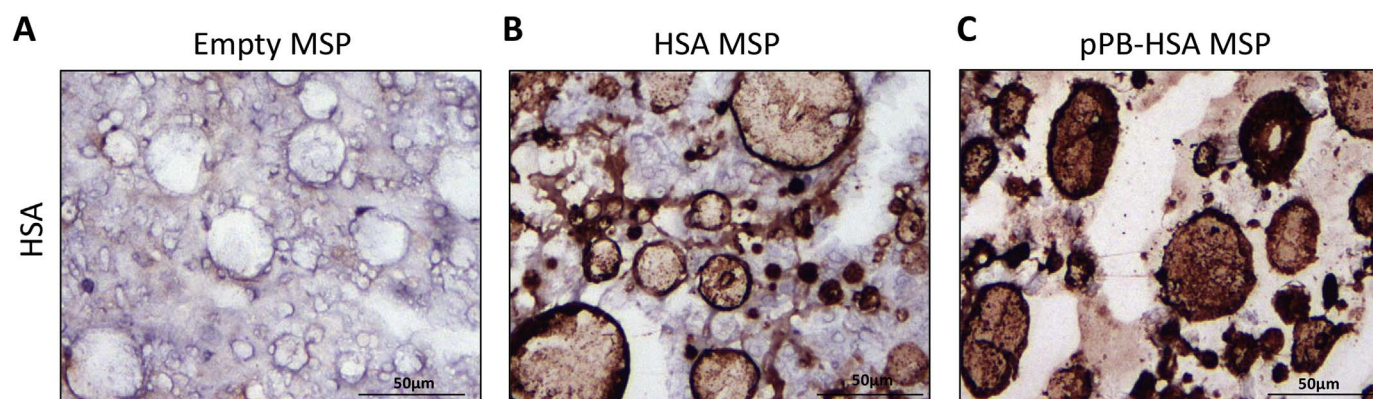


Fig. 4. Immunohistochemical staining for HSA of skin tissue samples at 7 days after injection. These samples were obtained at the subcutaneous injection site of the microspheres (MSP). MSP contained either (A) no protein, (B) HSA or (C) pPB-HSA.

this concentration at day 7 was associated with antibody formation, while antibody formation was prevented with the mouse albumin-based carrier.

In an attempt to correlate the *in vitro* release of pPB-HSA from microspheres and the estimated *in vivo* infusion-rate, based on the steady state concentration in plasma and the plasma clearance, we calculated release rates of 4.5%/day and 0.2%/day, respectively. This yields approximately a 20-fold lower value in the *in vivo* situation. According to Cardot and Tomic a linear *in vitro* - *in vivo* correlation only holds true when either drug dissolution or release from the formulation are the sole limiting factors for the systemic absorption [28]. In our studies, multiple factors might have contributed to the limitation in the *in vivo* infusion-rate of pPB-HSA, which will be discussed in more detail below.

The release of any drug from a subcutaneous depot occurs, when dissolved, within the subcutaneous tissue (or hypodermis) predominantly by diffusion or convection. The anatomy and micro-environment of the hypodermis can largely affect the release and transport of the drug [29]. Firstly, components of the subcutaneous extracellular matrix including collagens, noncollagenous glycoproteins, hyaluronic acid and chondroitin, heparan or dermatan sulfates can interfere with locally dissolved drugs and impede their passage to the circulation [30]. Such interference can happen in several ways, for example by electrostatic or (non-) specific interactions with the released protein drug. This ultimately leads to the formation of charged and/or large complexes that are unable to diffuse through the tissue and consequently accumulate subcutaneously instead [31,32]. Also, steric exclusion of the drug by the ECM can play a role, causing not only limited diffusion, but might also influence the solubility of the protein

drug [33]. Secondly, other microenvironmental parameters including the ionic composition and the pH of the injection site could limit protein absorption and stability [30,34]. Lastly, the uptake of drug in the systemic circulation can be reduced due to degradation of the protein at the injection site by the presence of proteases in the interstitial fluid [35].

After diffusion through the hypodermis, the released drug can reach the systemic circulation *via* local semipermeable capillaries or by lymphatic vessels, depending on the size of the protein. When the sustained release formulation is subcutaneously injected, the pressure in the interstitial fluid is increased. As compensatory mechanism, the local lymphatic flow is stimulated in order to transport excess of fluid into the lymphatic system. Consequently, more macromolecules with a diameter of up to 100 nm can be taken up, including pPB-HSA (which we assume to have a diameter of < 25 nm [36]), and eventually these molecules will be delivered to the bloodstream [37,38]. However, in mice Wu et al. demonstrated a limited uptake of a similar protein, *i.e.* bovine serum albumin, into the lymphatics following subcutaneous injection, thereby causing lower drug plasma concentrations [39]. Another reason could be pre-systemic metabolism of the drug which may occur in the draining lymphatics before reaching the circulation [35]. Such parameters cannot be easily mimicked *in vitro*. In summary, the *in vitro* studies are oversimplified as compared to the *in vivo* circumstances, which is clearly illustrated by our data. Recently, Kinnunen et al. made the first step towards an *in vitro* model that provides a better representation of subcutaneous conditions [40] and this model potentially yields better correlations with *in vivo* data in future studies.

Despite the expected discrepancy between the *in vitro* and *in vivo*

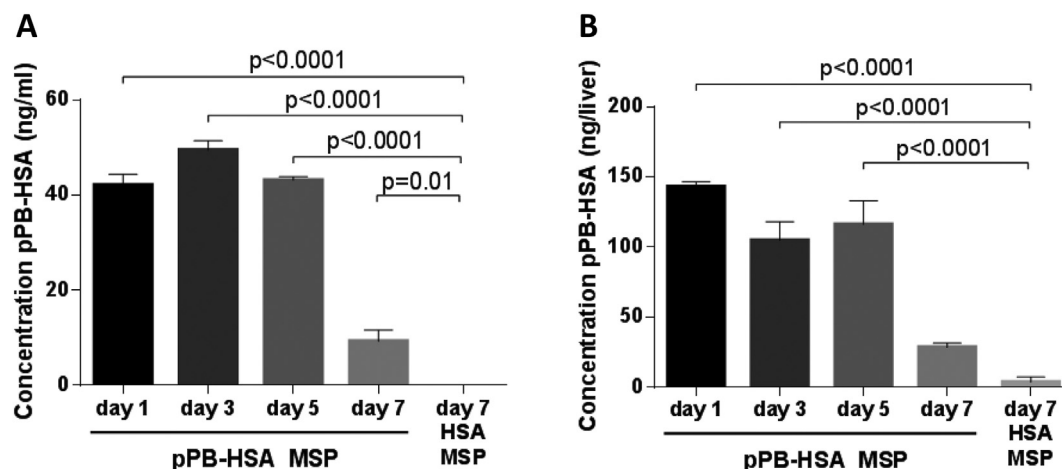
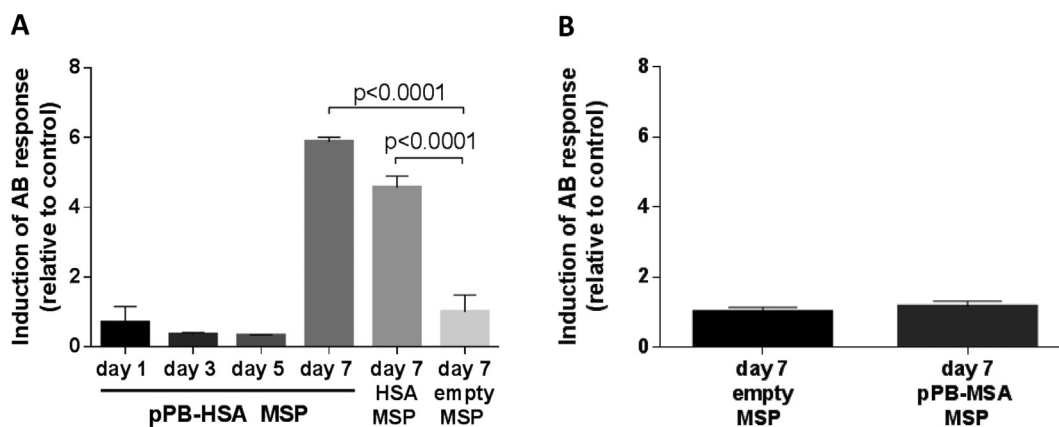


Fig. 5. Concentration of pPB-HSA in (A) plasma and (B) livers of Mdr2 -/- mice that received microspheres (MSP) subcutaneously for either 1, 3, 5 or 7 days containing pPB-HSA or HSA (only after 7 days) as determined with ELISA.



**Fig. 6.** Antibody (AB) response in plasma of Mdr2  $-/-$  mice that received microspheres loaded with either (A) pPB-HSA, HSA or no protein at 1, 3, 5 or 7 days after injection, or (B) pPB-MSA or no protein at 7 days after injection as measured by ELISA (statistics were performed using the unpaired student *t*-test). The control group consisted of mice injected with empty MSP. Note that an antibody-response was only present when levels exceeded the background levels in the control group.

release, we were able to show protein release and measured pPB-HSA at a plasma steady state concentration of approximately 45 ng/mL during 5 days after injection (Fig. 5A), a sound result in view of the extremely low *in vivo* half-life of 40 min. It is noteworthy that the calculated half-life might be an overestimation, as the PDGFR is most likely expressed at a lower level in the acute CCL<sub>4</sub>-model than in the more clinical relevant Mdr2  $-/-$  model, mimicking many disease features seen in human cirrhotic patients as well. Furthermore, a comparable concentration profile was demonstrated in the fibrotic liver as our target organ, in which the PDGFR-receptor was highly expressed, with a steady state concentration of  $121 \pm 28.3$  ng/liver within 1 day after injection. Whether this concentration is sufficient to reach therapeutic levels would depend on the potency of the attached antifibrotic compound.

Several studies showed the receptor selectivity of PDGFR-targeted constructs in different animal models [18,41,42]. With the use of I<sup>125</sup>-labeled pPB-HSA we confirmed the specific accumulation of this particular construct in mice suffering from acute liver fibrogenesis (Fig. 1). Because of the confirmation of the specific accumulation and the limited accumulation found in other organs (between 0.2 and 2.6%), we did not consider any accumulation in off-target organs in the pharmacokinetic study in the Mdr2  $-/-$  model.

The rapid decline in plasma concentration after 7 days was not anticipated, based on the pseudo zero-order *in vitro* release kinetics (Fig. 2B) and the presence of protein in the microspheres *in vivo* 7 days after injection (Fig. 4). We therefore hypothesized that this decline might be induced by antibody formation in mice against the human albumin-based carrier. Indeed, we demonstrated low antibody levels during the first 5 days, drastically increasing at day 7, which paralleled the decline in plasma and liver levels of pPB-HSA (Figs. 5, 6A). As part of the adaptive immune defense, B cells produce immunoglobulin antibodies against an antigen, *i.e.* a foreign protein like pPB-HSA or HSA in mice, upon prolonged exposure. The induced antibodies form complexes with pPB-HSA or HSA that are ultimately eliminated by the complement system [43].

Eventually, the induction of the immune response was successfully circumvented by replacing human albumin with mouse albumin (Fig. 6B), thereby creating a non-immunogenic drug carrier pPB-MSA. This alternative approach proved that the antibody formation was directed against the albumin part of pPB-HSA, and not against the pPB targeting moieties or the crosslinking domain. We now constructed a drug carrier that is compatible with our polymeric microsphere formulation and applicable for chronic administration of proteins.

In conclusion, we demonstrated that PDGFR-targeted albumin was released *in vivo* from the subcutaneously injected polymeric microspheres using hydrophilic multi-block copolymers composed of poly(L-

lactide) and poly ethylene glycol/poly( $\epsilon$ -caprolactone) blocks. pPB-HSA was detectable in the plasma and in the fibrotic liver up to 7 days after injection. This implies that sustained release microsphere formulations composed of these polymers are suitable for the parenteral delivery of therapeutic proteins and might constitute a realistic option for future application in chronic diseases such as liver fibrosis, bearing in mind that the origin of the potential therapeutic protein should be complementary to the species used as model. Future research should focus on pharmacodynamic aspects of the drug formulation, by incorporating the PDGFR-targeted albumin-based drug carrier coupled to an antifibrotic drug, thereby directing towards the clinical application of this combined delivery system ensuring sustained release of targeted therapeutic proteins.

## Acknowledgements

The authors thank Herman Steen (BiOrion Technologies B.V., Groningen) for providing pPB-HSA, Marlies Schippers (Department of Pharmacokinetics, Toxicology and Targeting, University of Groningen) and Marjolein van der Putten (student Pharmacy, University of Groningen) for their practical contributions, and Imco Sibum (Department of Pharmaceutical Technology and Biopharmacy, University of Groningen) for his assistance with the scanning electron micrographs. This research was performed in the framework of the Transition II and Peaks 2011 (Transitie II en Pieken 2011) subsidy program of The Northern Netherlands Provinces alliance (Samenwerkingsverband Noord-Nederland), and financially supported by the Province of Groningen (T2002), the municipality of Groningen and The Netherlands Institute for Regenerative Medicine, and the ERC Advanced Grant FIBROIMAGING to Detlef Schuppan.

## Appendix A. Supplementary data

Supplementary data to this article can be found online at <https://doi.org/10.1016/j.jconrel.2017.11.029>.

## References

- [1] A.C. Anselmo, S. Mitragotri, An overview of clinical and commercial impact of drug delivery systems, *J. Control. Release* 190 (2014) 15–28.
- [2] M.W. Tibbitt, J.E. Dahlman, R. Langer, Emerging frontiers in drug delivery, *J. Am. Chem. Soc.* 138 (2016) 704–717.
- [3] V.W. Steinijans, Pharmacokinetic characterization of controlled-release formulations, *Eur. J. Drug Metab. Pharmacokinet.* 15 (1990) 173–181.
- [4] S. Freitas, H.P. Merkle, B. Gander, Microencapsulation by solvent extraction/evaporation: reviewing the state of the art of microsphere preparation process technology, *J. Control. Release* 102 (2005) 313–332.
- [5] R. Vaishya, V. Khurana, S. Patel, A.K. Mitra, Long-term delivery of protein therapeutics, *Expert Opin. Drug Deliv.* 12 (2015) 415–440.



- [6] M. Cohen-Naftaly, S.L. Friedman, Current status of novel antifibrotic therapies in patients with chronic liver disease, *Therap. Adv. Gastroenterol.* 4 (2011) 391–417.
- [7] S.L. Friedman, Liver fibrosis - from bench to bedside, *J. Hepatol.* 38 (2003) s38–s53.
- [8] D. Schuppan, N.H. Afdhal, Liver cirrhosis, *Lancet* 371 (2008) 838–851.
- [9] W.Z. Mehal, D. Schuppan, Antifibrotic therapies in the liver, *Semin. Liver Dis.* 35 (2015) 184–198.
- [10] A. Said, M.R. Lucey, Liver transplantation: an update 2008, *Curr. Opin. Gastroenterol.* 24 (2008) 339–345.
- [11] Y. Popov, D. Schuppan, Targeting liver fibrosis: strategies for development and validation of antifibrotic therapies, *Hepatology* 50 (2009) 1294–1306.
- [12] D. Schuppan, Y.O. Kim, Evolving therapies for liver fibrosis, *J. Clin. Invest.* 123 (2013) 1887–1901.
- [13] W.R. Strohl, Fusion proteins for half-life extension of biologics as a strategy to make biobetters, *BioDrugs* 29 (2015) 215–239.
- [14] G. Walsh, Biopharmaceutical benchmarks 2014, *Nat. Biotechnol.* 32 (2014) 992–1000.
- [15] R. Bansal, J. Prakash, E. Post, L. Beljaars, D. Schuppan, K. Poelstra, Novel engineered targeted interferon-gamma blocks hepatic fibrogenesis in mice, *Hepatology* 54 (2011) 586–596.
- [16] E. Borkham-Kamphorst, E. Kovalenko, C.R.C. van Roeyen, N. Gassler, M. Bomble, T. Ostendorf, J. Floege, A.M. Gressner, R. Weiskirchen, Platelet-derived growth factor isoform expression in carbon tetrachloride-induced chronic liver injury, *Lab. Invest.* 88 (2008) 1090–1100.
- [17] L. Wong, G. Yamasaki, R.J. Johnson, S.L. Friedman, Induction of beta-platelet-derived growth factor receptor in rat hepatic lipocytes during cellular activation in vivo and in culture, *J. Clin. Invest.* 94 (1994) 1563–1569.
- [18] L. Beljaars, B. Weert, A. Geerts, D.K.F. Meijer, K. Poelstra, The preferential homing of a platelet derived growth factor receptor-recognizing macromolecule to fibroblast-like cells in fibrotic tissue, *Biochem. Pharmacol.* 66 (2003) 1307–1317.
- [19] S. Mao, C. Guo, Y. Shi, L.C. Li, Recent advances in polymeric microspheres for parenteral drug delivery—part 1, *Expert Opin. Drug Deliv.* 9 (2012) 1161–1176.
- [20] M. Stanković, J. Tomar, C. Hiemstra, R. Steendam, H.W. Frijlink, W.L.J. Hinrichs, Tailored protein release from biodegradable poly( $\epsilon$ -caprolactone-PEG)-b-poly( $\epsilon$ -caprolactone) multiblock-copolymer implants, *Eur. J. Pharm. Biopharm.* 87 (2014) 329–337.
- [21] M. Stanković, C. Hiemstra, H. de Waard, J. Zuidema, R. Steendam, H.W. Frijlink, W.L.J. Hinrichs, Protein release from water-swelling poly(D,L-lactide-PEG)-b-poly( $\epsilon$ -caprolactone) implants, *Int. J. Pharm.* 480 (2015) 73–83.
- [22] N. Teekamp, F. Van Dijk, A. Broesder, M. Evers, J. Zuidema, R. Steendam, E. Post, Polymeric microspheres for the sustained release of a protein-based drug carrier targeting the PDGFR $\beta$ -receptor in the fibrotic kidney, *Int. J. Pharm.* 534 (2017) 229–236.
- [23] M. Stanković, H. de Waard, R. Steendam, C. Hiemstra, J. Zuidema, H.W. Frijlink, W.L.J. Hinrichs, Low temperature extruded implants based on novel hydrophilic multiblock copolymer for long-term protein delivery, *Eur. J. Pharm. Sci.* 49 (2013) 578–587.
- [24] L. Beljaars, G. Molema, D. Schuppan, A. Geerts, P. De Bleser, B. Weert, D. Meijer, K. Poelstra, Successful targeting to rat hepatic stellate cells using albumin modified with cyclic peptides that recognize the collagen type VI receptor, *J. Biol. Chem.* 275 (2000) 12743–12751.
- [25] Y. Popov, E. Patsenker, P. Fickert, M. Trauner, D. Schuppan, Mdr2 (Abcb4) – / – mice spontaneously develop severe biliary fibrosis via massive dysregulation of pro- and antifibrogenic genes, *J. Hepatol.* 43 (2005) 1045–1054.
- [26] J. Proost, MULTIFIT: An Interactive Program for Non-Linear Curve-fitting of Several Pharmacokinetic Models and Mathematical Functions, (1992).
- [27] PhRMA, Medicines in Development: Biologics, Washington, DC (2013).
- [28] J.M. Cardot, I. Tomic, In vitro in vivo correlation basis and application to slow release injectable formulation, *Farmacia* 63 (2015) 781–791.
- [29] J.R. Weiser, W.M. Saltzman, Controlled release for local delivery of drugs: barriers and models, *J. Control. Release* 190 (2014) 664–673.
- [30] H.M. Kinnunen, R.J. Mørn, Improving the outcomes of biopharmaceutical delivery via the subcutaneous route by understanding the chemical, physical and physiological properties of the subcutaneous injection site, *J. Control. Release* 182 (2014) 22–32.
- [31] H. Mach, S.M. Gregory, A. Mackiewicz, S. Mittal, A. Laloo, M. Kirchmeier, M. Shameem, Electrostatic interactions of monoclonal antibodies with subcutaneous tissue, *Ther. Deliv.* 2 (2011) 727–736.
- [32] Y. Yao, K. Hashimoto, K. Takahara, I. Kato, Insulin binds to type V collagen with retention of mitogenic activity, *Exp. Cell Res.* 194 (1991) 180–185.
- [33] T.C. Laurent, H. Persson, On the interaction between polysaccharides and other macromolecules III. The use of hyaluronic acid for the separation of macromolecules in the ultracentrifuge, *Biochim. Biophys. Acta* 78 (1963) 360–366.
- [34] F. Cugia, M. Monduzzi, B.W. Ninham, A. Salis, Interplay of ion specificity, pH and buffers: insights from electrophoretic mobility and pH measurements of lysozyme solutions, *RSC Adv.* 3 (2013) 5882–5888.
- [35] W.F. Richter, S.G. Bhansali, M.E. Morris, Mechanistic determinants of biotherapeutics absorption following SC Administration, *AAPS J.* 14 (2012) 559–570.
- [36] M.L. Ferrer, R. Duchowicz, B. Carrasco, J.G. de la Torre, A.U. Acuña, The conformation of serum albumin in solution: a combined phosphorescence depolarization-hydrodynamic modeling study, *Biophys. J.* 80 (2001) 2422–2430.
- [37] E. Hommel, E.R. Mathiesen, K. Aukland, H.H. Parving, Pathophysiological aspects of edema formation in diabetic nephropathy, *Kidney Int.* 38 (1990) 1187–1192.
- [38] C.J.H. Porter, G.A. Edwards, S.A. Charman, Lymphatic transport of proteins after s.c. injection: implications of animal model selection, *Adv. Drug Deliv. Rev.* 50 (2001) 157–171.
- [39] F. Wu, S.G. Bhansali, M. Tamhane, R. Kumar, L.A. Vathy, H. Ding, K.-T. Yong, E.J. Bergey, P.N. Prasad, M. Morris, Noninvasive real-time fluorescence imaging of the lymphatic uptake of BSA-IRDye 680 conjugate administered subcutaneously in mice, *J. Pharm. Sci.* 101 (2012) 1744–1754.
- [40] H.M. Kinnunen, V. Sharma, L.R. Contreras-Rojas, Y. Yu, C. Alleman, A. Sreedhara, S. Fischer, L. Khawli, S.T. Yohe, D. Bumbaca, T.W. Patapoff, A.L. Daugherty, R.J. Mørn, A novel in vitro method to model the fate of subcutaneously administered biopharmaceuticals and associated formulation components, *J. Control. Release* 214 (2015) 94–102.
- [41] R. Bansal, T. Tomar, A. Ostman, K. Poelstra, J. Prakash, Selective targeting of interferon  $\gamma$  to stromal fibroblasts and pericytes as a novel therapeutic approach to inhibit angiogenesis and tumor growth, *Mol. Cancer Ther.* 11 (2012) 2419–2428.
- [42] J. Prakash, E. de Jong, E. Post, A.S.H. Gouw, L. Beljaars, K. Poelstra, A novel approach to deliver anticancer drugs to key cell types in tumors using a PDGF receptor-binding cyclic peptide containing carrier, *J. Control. Release* 145 (2010) 91–101.
- [43] R. Warrington, W. Watson, H.L. Kim, F. Antonetti, An introduction to immunology and immunopathology, *Allergy, Asthma Clin. Immunol.* 7 (2011) S1.